

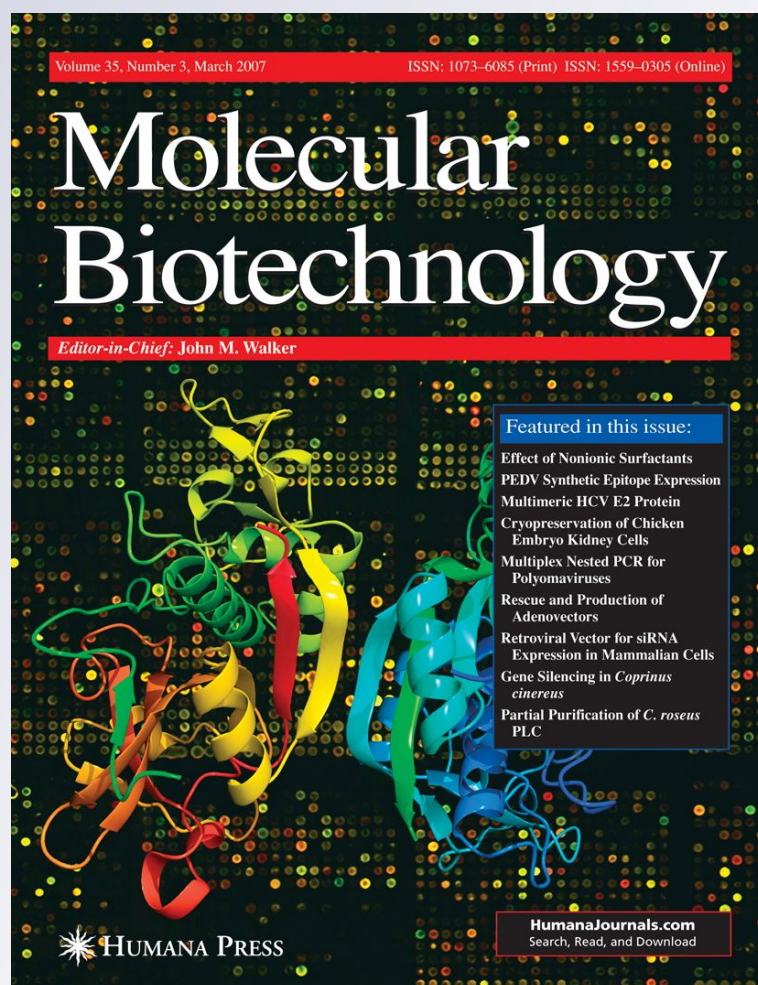
# Transfection Efficiency Along the Regenerating Soleus Muscle of the Rat

**Magdolna Kósa & Ernő Zádor**

**Molecular Biotechnology**  
Part B of Applied Biochemistry and  
Biotechnology

ISSN 1073-6085

Mol Biotechnol  
DOI 10.1007/s12033-012-9555-2



**Your article is protected by copyright and all rights are held exclusively by Springer Science+Business Media, LLC. This e-offprint is for personal use only and shall not be self-archived in electronic repositories. If you wish to self-archive your work, please use the accepted author's version for posting to your own website or your institution's repository. You may further deposit the accepted author's version on a funder's repository at a funder's request, provided it is not made publicly available until 12 months after publication.**

# Transfection Efficiency Along the Regenerating Soleus Muscle of the Rat

Magdolna Kósa · Ernő Zádor

© Springer Science+Business Media, LLC 2012

**Abstract** We investigated the efficiency of a single plasmid transfection along the longitudinal axis of the regenerating soleus of young rats. This also reflected transfection efficiency along the fibers because the soleus is a nearly fusiform muscle in young animals. The complete regeneration was induced by notexin and the transfection was made by intramuscular injection of enhanced green fluorescent protein- or *Discosoma* red-coding plasmids after 4 days. One week after transfection the number of transfected fibers was higher at the place of injection (i.e., in the muscle belly) and lower or absent at the ends of the muscle. The inspection of longitudinal sections and neuromuscular endplates indicated that one of the reasons of uneven transfection might be the shortness of transfected myotubes and the other reason might be the limit of diffusion of transgenic proteins from the expressing nuclei. As a result, the efficiency of transfection in the whole regenerating muscle was much lower than it could be estimated from the most successfully transfected part.

**Keywords** Transfection efficiency · Fiber length · Regeneration · Notexin · Skeletal muscle

## Introduction

Since the first report of *in vivo* transfection of mouse skeletal muscle [1], a number of methods have been developed in order to improve transgene introduction into the manipulated organ. These techniques utilized electroporation [2], treatment with hyaluronidase [3, 4], ultrasound [5], polymers [6, 7], gene gun [8], and hydrodynamic plasmid delivery [9]. Although these efforts remarkably improved efficiency but further studies might still help to optimize transfection for therapeutic and experimental use. One of the main questions of muscle transfection is that will the transgene be expressed along the fibers? Muscle fibers are synthitia containing hundreds or thousands of nuclei, most of these are not likely to take up foreign DNA uniformly. This results in an uneven distribution of the transgene which makes difficult to measure transfection efficiency and the transgene expression along the fibers.

When investigating transfection efficiency, many articles compare cross sections from certain parts of the muscle [3, 4] or measure the amount of the expressed transgenic protein in the whole muscle homogenate [2, 7]. Both of these methods have drawbacks; since the transversal sections do not reveal transfection efficiency along the muscle, and measuring transgenic protein in the whole muscle homogenate misses the transgene distribution and the morphological effect. However, only a few laboratories have investigated transfection efficiency on longitudinal sections [10] and in whole-mount preparations of mice muscles [2, 10, 11]. They showed that the expression of the transgene was restricted to the place of transfection, meanwhile others found that the expressed GFP diffused along single fibers after injection [12]. These results show variance, although come from mice, which have a shorter muscle than that of rat. Therefore it is relevant to study

---

M. Kósa · E. Zádor (✉)  
Department of Biochemistry, Faculty of Medicine, University  
of Szeged, Dom ter 9, Szeged 6720,  
Hungary  
e-mail: zador.erno@med.u-szeged.hu

M. Kósa  
e-mail: kosa.magdolna@med.u-szeged.hu  
URL: <http://www.biochem.szote.u-szeged.hu>

how the transfection efficiency changes along the muscle of larger animals, i.e., of rat.

The regenerating skeletal muscle of the rat can be transfected efficiently by intramuscular injection of naked plasmid DNA without any further manipulations [10]. Such transfection is effective in 1 % of the fibers, as it has been estimated from transversal sections of the central part of the regenerating rat soleus muscle [13, 14]. Our aim was to further characterise the transfection efficiency along the whole regenerating rat soleus. This was particular interesting because previously we found that the expression of certain transgenes in only a few fibers stimulates regeneration in the whole soleus muscle [15, 16]. We have seen impressive muscle growth, apparently due to autocrine–paracrine effect. In order to describe such mechanism, it is important to characterise the efficiency of the transfection used in the same muscle regeneration. In connection with this, we also aimed to study the fiber length in the regenerating soleus compared to that of the normal muscle. This question has relevance since the fiber length is nearly equal to muscle length in the young soleus [17]. Similarly, in regeneration, the fiber length could also determine transfection efficiency along the soleus.

## Materials and Methods

### Animal Treatment and Freeze Sectioning

Male Wistar rats (320–390 g) were treated as described by Zádor et al. [18]. In brief, animals were anesthetized by intraperitoneal injection of 4 % chloral hydrate (1 ml/100 g bodyweight). After a small incision on the lateral side of the left hind limb, the soleus muscle was explored and injected with 0.15 ml notexin (100 µg/ml solution; Sigma-Aldrich) which induced a complete necrosis in the whole muscle, abolishing a number of muscle specific markers, and followed by an even regeneration in the whole soleus [13–16, 19]. No intact or partially damaged adult fibers were found i.e., after 4 days of notexin injection. We found this particularly important since gradation of injury made more difficult to standardize transfection therefore to evaluate the result. After the wound was closed animals could move, eat, and drink according to their demands. For transfection the soleus was re-explored 4 days after the notexin treatment and injected at the mid-belly with a total volume of 50-µl plasmid (1 µg/µl; 20 % sucrose in DEP water) by Hamilton Microsyringe. The central part of the soleus was chosen for injection to make easier to monitor plasmid distribution along the muscle toward the proximal and distal ends. This was not the most efficient way of transfection, a higher efficacy could be achieved by piercing the needle longitudinally from

proximal-to-distal end into the soleus, then withdrawing it with continuously injecting the plasmid [10]. However such perfusion often resulted in random transfected segments along the muscle and fibers which hampered the statistical analysis of distribution therefore we did not apply it. On the 11th day of notexin-induced regeneration and 7 days after transfection at mid-belly, the muscles were dissected, fixed on small wooden sticks by thread, cooled in liquid nitrogen chilled in isopentane and stored at  $-70^{\circ}\text{C}$ . For acetylcholine esterase (AChE) staining, before the 11th day of regeneration, muscles were removed on the 5th or 7th days after notexin treatment. Animals were killed with an overdose of chloral hydrate. Experiments with animals were approved by the Ethical Committee of Animal Treatment of the Medical Faculty of the University of Szeged.

Frozen soleus muscles were cut into 6 approximately equal segments. After embedding the segments in Tissue Tek, 10-µm thin frozen cross sections were performed by Reichert-Jung Cryostat. Native sections were air-dried on glass slides and stored at  $-25^{\circ}\text{C}$  until microscopic evaluation or staining.

### Plasmids

pEGFP (3.4 kb) and pDsRed (3.3 kb) plasmids (Clontech) were used for transfection. Driven by CMV promoter they expressed green or red fluorescent proteins in myofibers which allowed the direct investigation of transgene expression under fluorescent microscope. Plasmids were purified by Qiagen Plasmid Maxi Kit from 100-ml bacterium culture. The concentration of purified plasmid was measured and its quality assessed by the absorbance ratio at 260/280 nm on NanoDrop ND-1000. This ratio was between 1.78 and 1.87 for both plasmids. The quality of the purified plasmid preparations was also checked on agarose gel.

### Calculating Transfection Efficiency

Results presented here have been collected from 11 successfully transfected muscles from which 6 were injected with pEGFP, and 5 with pDsRed. An advantage of the green and red fluorescent proteins is the easy visualization without further staining procedures, difficulty in fiber identification happens only in extreme cases (very low emission vs. background autofluorescence; high emission—light contamination in the surrounding fibers).

The number of transfected fibers was counted on 2–4 sections from each of the 6 segments on Nikon Labophot-2 fluorescent microscope (RO or FITC filter) equipped with Olympus DP71 camera connected to computer with Cell\* B imaging software.

## Staining Soleus Sections

Hematoxylin-eosin staining was performed to prove the stage of regeneration by measuring fiber cross-sectional areas (CSA) and to count myofibers. AChE histochemistry was prepared after Tago et al. [20] but after washing sections with 3 % H<sub>2</sub>O<sub>2</sub>, they were rinsed in PBS two times and incubated in ethopropazine ( $2 \times 10^{-4}$  M) for 30 min in dark to block aspecific cholinesterase activity [21]. Neuromuscular junctions (NMJs) were counted under light microscope. Schematic drawings were prepared by MS Office PowerPoint 2007.

## Counting Fibers Associated with AChE Positive Staining

AChE is bound to the basal lamina in the post-synaptical cleft [22, 23] so it is an indicator of the NMJs. The other AChE-stained phenomena (i.e., myotendinous junctions (MTJs) and proprioceptors [24, 25] have different morphology. AChE was stained on at least 4 cross sections from each segment of six muscles, and those with the highest number of AChE were selected and compared. Sections spanned at least 40–100  $\mu$ m distance.

## Statistics

Comparison of the means were done by ANOVA and Bonferroni post-hoc test (Software: SPSS 15.0), data was presented by SPSS 15.0.

## Results

### Transfection Efficiency Along the Muscle

The transfection was evaluated at 7 days after plasmid injection and 11 days after notexin injection. Transfected fibers were easy to distinguish from non-transfected ones by their high fluorescence, they stood alone or associated in groups as it was reported by Doh et al. [11]. Interestingly, the fluorescence intensity of transfected fibers changed on consecutive sections even within one segment (Fig. 1). The maximum number of transfected fibers varied between 10 and 86 per section. There was no significant difference between the enhanced green fluorescent protein (EGFP) and Discosoma red (DsRed plasmids) in respect of transfection efficiency in the same segments (Fig. 2). Sections with the highest transfection rate were found in segments 2–4, and only one muscle had its peak transfection efficiency in the 5th segment. Data from the individual muscles (Table 1) also show a decline in the number of transfected fibers toward the proximal and the distal ends. In summary, EGFP

in the 3rd and 4th segments, while DsRed in the 2nd and 3rd segments had significantly more transfected fibers than in the first and the last segments (Fig. 2). This correlated well with the place of injections at the muscle mid-bellies. However, it is worth to note that the transfection was also restricted near to muscle ends, i.e., in muscles c and i (Table 1) not only at the mid-belly (segments 3–4).

The soleus is a nearly fusiform muscle [17] which suggests that if the transfection is partial along the muscle, the transfected nuclei are also not evenly distributed along the fibers. However, an average soleus contains up to 3,000 fibers in the central segments [14, 16], while only about 1,000 fibers were found in the terminal areas (data not shown). Also, at the time of transfection, the myotubes might be shorter than later in regeneration [26]. Furthermore, it is possible that the regenerating myotubes do not fuse with each other but stay divided by MTJs [27].

### Staining of Neuromuscular Endplates (NME) on Longitudinal Section

In order to find out whether the uneven transfection along the muscle was due to shortness of myotubes at the time of the intramuscular plasmid injection, we stained NME for AChE. In mammals, each muscle fiber is innervated only by one endplate, therefore, if myotubes did not fuse with each other in regeneration, the position and the number of the endplates would be the same as in the normal muscle. Since innervation is a prerequisite for the successful regeneration [28] the position of endplates should imply any major change in the average fiber length in the regenerating muscle.

The pattern of AChE positive endplates in 11-days regenerated transfected soleus was similar to that of the normal muscle, except, they were less organized and more diffused, i.e., they followed less even diagonal line on longitudinal sections than in the normal soleus. This diagonal line was a lateral view of the elliptical pattern of NMEs in the muscle mid-belly [29–31]. The number of NMEs in the different segments (Table 2) reveals that NMEs are central positioned in regenerating muscles as in the normal soleus. This suggests that fiber length is nearly restored by day 11 of regeneration. Accordingly, matured endplate potentials have been measured by others at this stage in the same type of regeneration of the soleus [32]. Therefore, the movement of plasmids and transgenic proteins is probably not limited by fiber length along the 11-days regenerating muscle. However, on longitudinal sections of 5-days regenerating soleus (1 day after transfection), the primitive fibers/myotubes were much shorter (Fig. 3) than at day 11 (when the transfection was inspected) or in the normal muscle [17]. This suggests that the efficient transfection in the full length of the 11-days regenerating muscle might be limited by the

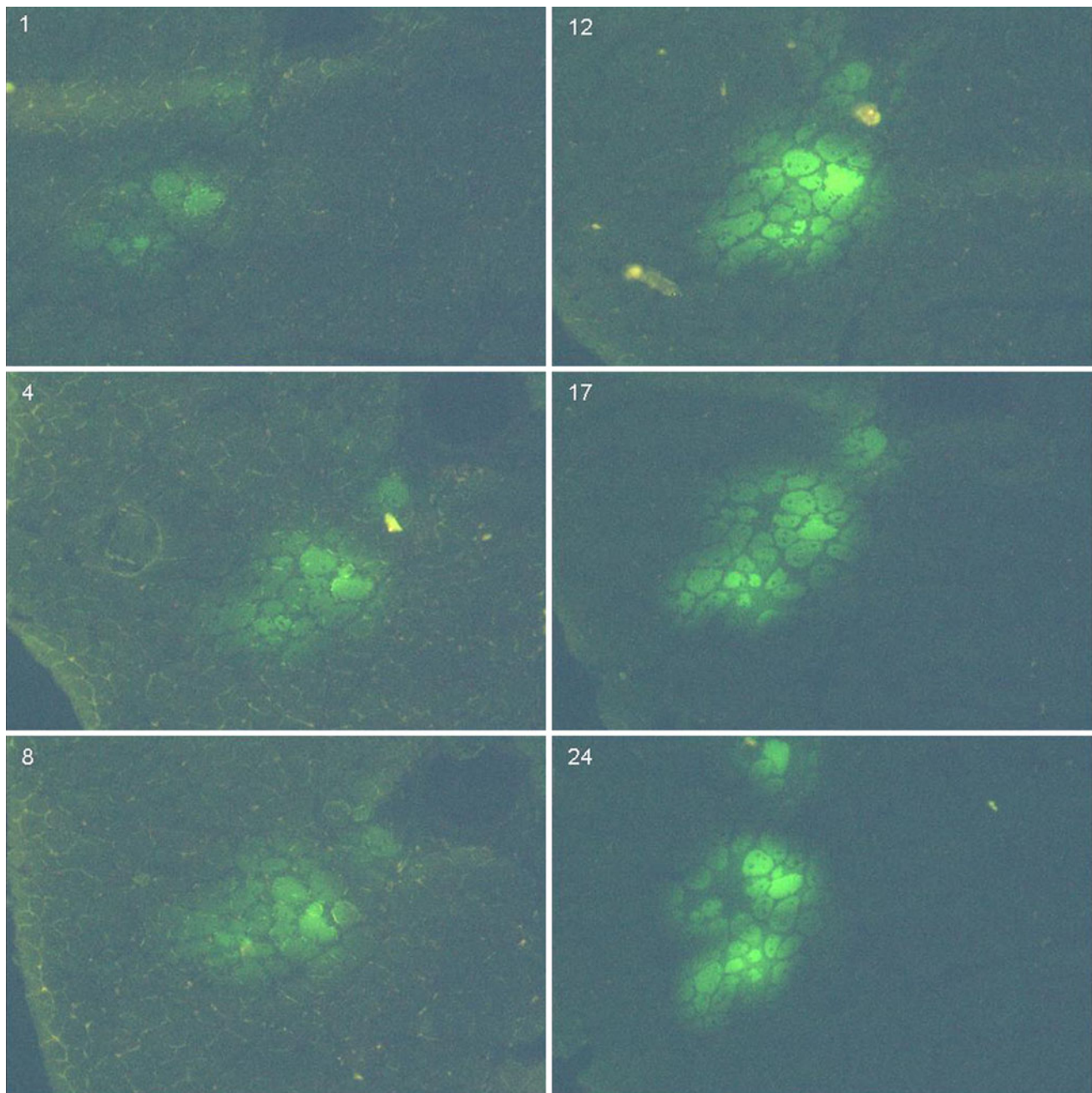


**Fig. 1** Consecutive transversal sections taken from one segment of regenerating soleus muscle transfected with EGFP. The order of 1–24 sections is indicated. Note that transfection intensity in many fibers changes already after a few sections therefore within a short distance

shortness of myotubes at day 4, at the time of transfection. Therefore, anatomical borders like position of transfected nuclei and myotube length at the time of transfection may limit transfection efficiency along the regenerating muscle.

### Discussion

Transversal sections taken systematically along the soleus muscle showed that the number of transfected fibers was

higher in the central parts and decreased toward the proximal and distal ends; this finding was independent of the used reporter genes. One of the explanations is that the transfected plasmids, the expressed RNAs, and proteins are not transported within muscle fibers. Indeed, in regenerating muscle, the young myotubes are divided by MTJs and later develop into longer fibers [27]. To monitor transfection along the fibers, we divided the fusiform soleus muscle in length into six equal segments (4–5 mm, 1/6 of muscle length). EGFP and DsRed expressions in the fibers

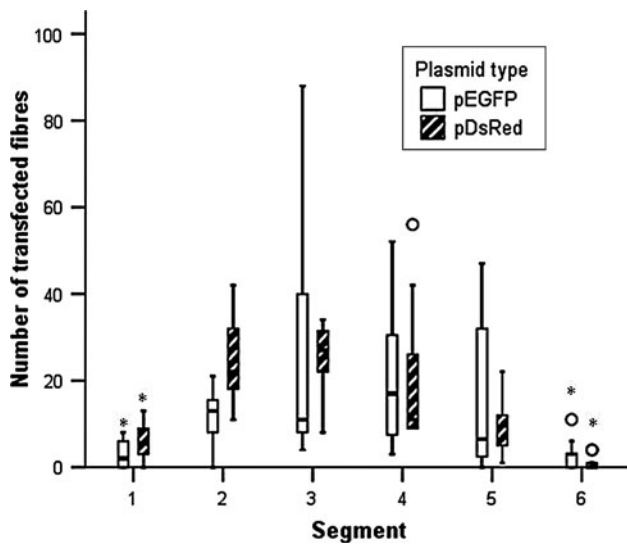


**Fig. 2** Summary of transfected fibers in segments of (pEGFP or pDsRed,  $n = 11$ ) transfected muscles. At each segment 2 vertical box plots demonstrate the transfected fiber counts. Empty boxes refer to muscles transfected with pEGFP, patterned ones to those with pDsRed. Length of boxes presents the interquartile range (IQR) computed from Tukey's hinges. Whisker caps indicate minimum and maximum values. Circles mark outlier values (more than 1.5 IQR's but <3 IQR's from the end of the box). There was no significant difference between pEGFP and pDsRed transfection efficiency within the same segment. Highest mean of transfected fibers is in segment 3 (both pEGFP and pDsRed). The peripheral segments 1 and 6 contain significant less fibers then segment 3 and 4 in case of pEGFP transfection and segment 2 and 3 in case of pDsRed transfection. Asterisks marks significant differences ( $p < 0.05$ ; Bonferroni post-hoc test)

declined already along a single segment. Such an uneven transgene expression has been reported previously along the fibers of mouse rectus femoris [11]. The distal and proximal fiber ends showed pronounced  $\beta$ -galactosidase expression 3–6 h after transfection which turned out to be somehow more evenly distributed along the fibers at 4 days after plasmid treatment. In another study, the transfected  $\beta$ -galactosidase exhibited segmental differences within the fibers of regenerating rat soleus muscles on serially cross and longitudinal sections [10]. This latter finding has not been supported by the whole-mount analysis of extensor digitorum longus muscles in mice, where the GFP occupied the whole fiber [33] and a similar observation was made after single fiber transfection [12].

To interpret the declining expression levels along the fibers, we should consider that plasmids are not homogeneously distributed along the entire muscle after being injected. Doh et al. [11] hypothesized that DNA could accumulate in “pockets” which could be responsible for the varying expression pattern. In our opinion, such pockets could be even more frequent in regenerating than in normal muscles, which often contain split fibers [34]. In addition,

**Table 1** Number of transfected fibers in the segments of 11 transfected muscles

| Muscle ID     | Segments |    |    |    |    |    |
|---------------|----------|----|----|----|----|----|
|               | 1        | 2  | 3  | 4  | 5  | 6  |
| <b>pEGFP</b>  |          |    |    |    |    |    |
| a             | 8        | 13 | 6  | 4  | 2  | 3  |
| b             | 5        | 13 | 51 | 49 | 22 | 6  |
| c             | 1        | 8  | 11 | 17 | 44 | 11 |
| d             | 0        | 21 | 86 | 39 | 9  | 0  |
| e             | 6        | 19 | 40 | 20 | 0  | 0  |
| f             | 0        | 0  | 10 | 9  | 4  | 3  |
| <b>pDsRed</b> |          |    |    |    |    |    |
| g             | 0        | 12 | 10 | 26 | 11 | 0  |
| h             | 8        | 18 | 31 | 11 | 6  | 0  |
| i             | 13       | 35 | 22 | 9  | 2  | 0  |
| j             | 8        | 37 | 38 | 49 | 21 | 1  |
| k             | 3        | 23 | 26 | 10 | 11 | 4  |

Data represents average number of transfected fibers on cross sections. Muscles transfected with pEGFP or pDsRed are shown separately. Note that transfection efficiency is different in each muscle, but the number of transfected fibers declines toward the muscle ends

**Table 2** Number of fibers associated with AChE positive NMJ staining in transfected soleus cross sections at day 11 of regeneration

| Muscle ID      | Segments |    |    |    |    |    |
|----------------|----------|----|----|----|----|----|
|                | 1        | 2  | 3  | 4  | 5  | 6  |
| a <sup>1</sup> | 0        | 0  | 66 | 91 | 11 | 5  |
| b <sup>1</sup> | 7        | 5  | 27 | 36 | 67 | 5  |
| c <sup>1</sup> | 4        | 2  | 21 | 55 | 18 | 1  |
| d <sup>1</sup> | 0        | 11 | 38 | 88 | 22 | 0  |
| e <sup>2</sup> | 4        | 0  | 0  | 82 | 37 | 3  |
| f <sup>2</sup> | 0        | 0  | 17 | 16 | 19 | 10 |

The highest numbers of NMJ associated fibers are in segments 3–5, in the muscle belly. The normal muscles also exhibit endplates in the central belly, therefore it is likely that transfected regenerating muscles have the similar innervation pattern to the normal soleus. <sup>1</sup> Muscles transfected with pEGFP and <sup>2</sup> with pDsRed

if we consider that 95 % of the plasmids degraded in the first 6 h in the interstitial space [35], the chance of long-term diffusion is indeed extremely low. Plasmids have to be incorporated next to the site of injection and this happens in case of only a few nuclei [12]. The nuclear resident plasmids express the transgene in the vicinity called myonuclear domain. We are not aware of transport mechanism that would span the fibers with transcribed RNA or translated proteins. Since fibers in mice muscles are smaller than in rat muscles, the transgene concentration can be equalized more efficiently in mice than in rat muscles [12, 33]. The distance of DNA-containing

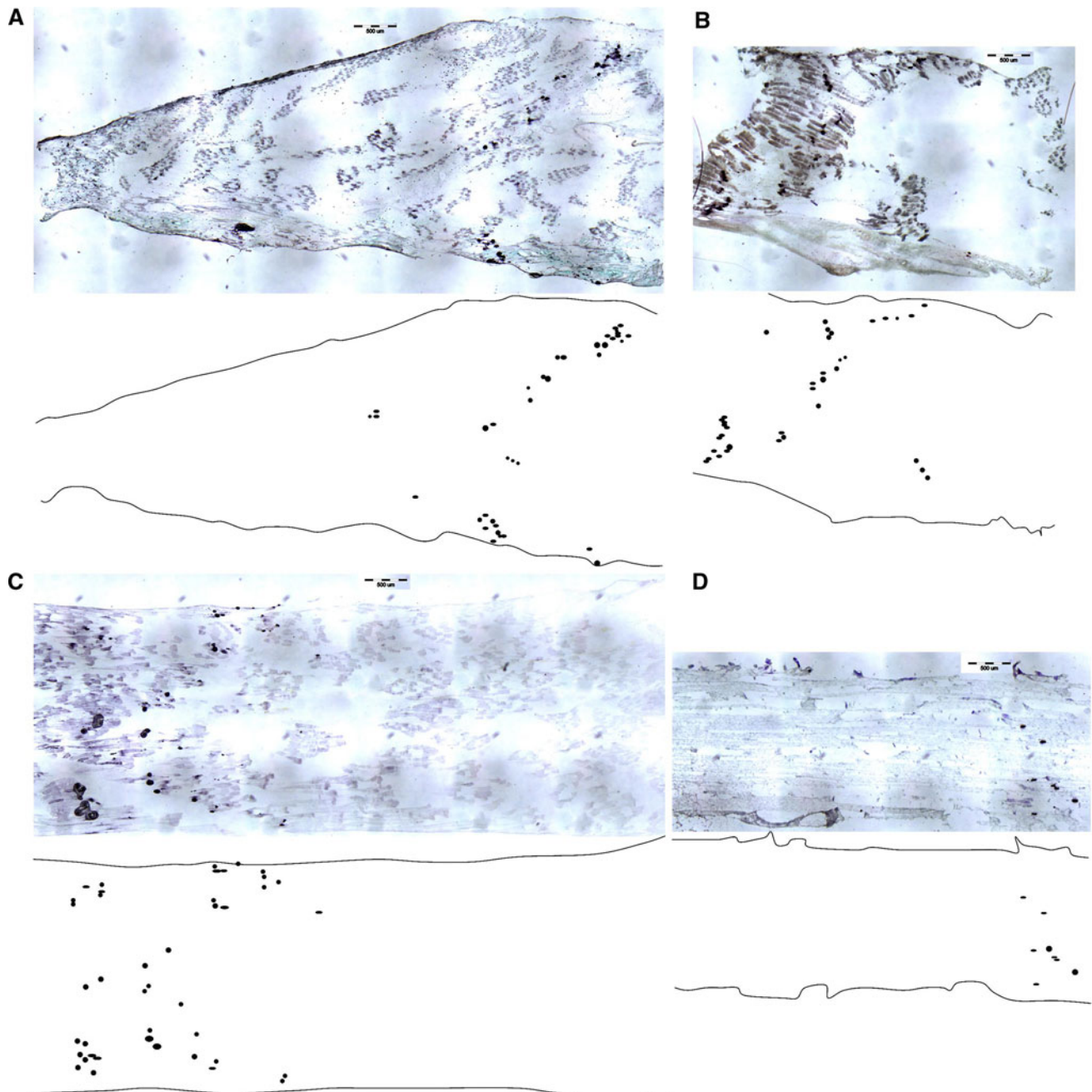


**Fig. 3** Images of AChE-stained longitudinal sections (magnification  $\times 40$ ) are composed to reconstruct a complete view of the section. A schematic drawing marks the AChE positive *endplates* under each section. Regenerating soleus on day 5 (**a**), day 7 (**b**) and day 11 (**c**),

and normal soleus (**d**). Note that the pattern and distribution of the NMJs are similar in normal and regenerating muscles, suggesting that by the time of established innervation (day 7–11) the fiber length is similar in both conditions (see table 2)

“pockets” from transfectable nuclei and the diffusion-limits of the expressed gene products seem to be plausible explanations for the uneven transgene distribution along the fibers.

The other explanation is that the myotubes were shorter at the time of transfection than at the time of monitoring of GFP expression. Plasmid injected to the central part of the regenerating soleus, had little chance to get to muscle ends

because the myotubes/young fibers were much shorter than the whole muscle length [26]. Later, when the young fibers fused with each other the transfected nuclei still remained on spot [36–40].

Since each fiber has one innervation in mammals [41], we used NMJs to test the fusion of myotubes as an indirect control of fiber length. If the myotubes did not fuse by day 11 of regeneration (when the transfection was inspected)

the number of NMJs would increase at muscle ends. On the contrary, if the myotubes managed to fuse, the NMJs should still be in the mid-belly like in the normal soleus [29]. Our results showed that the NMJs were approximately in the same position in the regenerating and normal muscles on longitudinal and cross sections. The innervation of most fibers is completed by day 7 of regeneration [32, 42], fibers interrupted by MTJs after this time are less likely to occur. We analyzed regenerating muscles at day 5, (1 day after transfection) and day 11 (when the transfection was inspected). We found that the fiber length was relatively short on day 5, it appeared longer at day 7 and even longer at day 11, almost as long as in the untreated soleus; though fiber CSAs were significantly behind that of normal muscles.

Therefore, as a consequence, we can say that the uneven distribution of transfection in the regenerating muscle is probably due to the fixed position of transfected nuclei and to the limited diffusion of the expressed transgenic proteins. The regional changing of transfection means that the efficiency can not be estimated accurately from one part of the muscle even if it is the most transfected part. This highlights the vagueness of assumption of transfection in skeletal muscle, especially in gene therapies applied in degenerative-regenerative disorders like Duchenne type muscle dystrophy. Considering that shape, pennation and anatomical structure in most muscles are more complicated than in the soleus, the estimation of transfection efficiency in other muscles looks even more dubious. Strategies aiming transfection of a certain percentage of fibers must count on this insecurity. Interestingly, our novel method, in which growth stimulation of the entire regenerating soleus is reached by transfection of only a few fibers with signal pathway inhibitors [15, 16], can overcome the low transfection efficiency. We must note that in this case the effect is probably also initiated from a smaller part of the muscle than it seemed previously.

**Acknowledgments** The publication is supported by the Hungarian National Development Agency, the European Union and co-funded by the European Social Fund. Project numbers: TÁMOP-4.2.2/B-10/1-2010-0012; TÁMOP-4.2.1/B-09/1/KONV-2010-0005.

## References

- Wolff, J., Malone, R., Williams, P., Chong, W., Acsadi, G., Jani, A., et al. (1990). Direct gene transfer into mouse muscle in vivo. *Science*, 247(4949), 1465–1468.
- Mir, L. M., Bureau, M. F., Gehl, J., Rangara, R., Rouy, D., Caillaud, J. M., et al. (1999). High-efficiency gene transfer into skeletal muscle mediated by electric pulses. *Proceedings of the National Academy of Sciences of the United States of America*, 96(8), 4262–4267.
- Molnar, M. J., Gilbert, R., Lu, Y. F., Liu, A. B., Guo, A., Larochelle, N., et al. (2004). Factors influencing the efficacy,

- longevity, and safety of electroporation-assisted plasmid-based gene transfer into mouse muscles. *Molecular Therapy*, 10(3), 447–455.
- Schertzer, J. D., Plant, D. R., & Lynch, G. S. (2006). Optimizing plasmid-based gene transfer for investigating skeletal muscle structure and function. *Molecular Therapy*, 13(4), 795–803.
- Lu, Q. L., Liang, H., Partridge, T., & Blomley, M. J. K. (2003). Microbubble ultrasound improves the efficiency of gene transduction in skeletal muscle in vivo with reduced tissue damage. *Gene Therapy*, 10, 396–405.
- Lemieux, P., Guerin, N., Paradis, G., Proulx, R., Chistyakova, L., Kabanov, A., et al. (2000). A combination of poloxamers increases gene expression of plasmid DNA in skeletal muscle. *Gene Therapy*, 7(11), 986–991.
- Chang, C., Choi, D., Kim, W. J., Yockman, J. W., Christensen, L. V., Kim, Y., et al. (2007). Non-ionic amphiphilic biodegradable PEG–PLGA–PEG copolymer enhances gene delivery efficiency in rat skeletal muscle. *Journal of Controlled Release*, 118(2), 245–253.
- Yang, N. S., Burkholder, J., Roberts, B., Martinell, B., & McCabe, D. (1990). In vivo and in vitro gene transfer to mammalian somatic cells by particle bombardment. *Proceedings of the National Academy of Sciences of the United States of America*, 87(24), 9568–9572.
- Zhang, G., Budker, V., Williams, P., Subbotin, V., & Wolff, J. A. (2001). Efficient expression of naked dna delivered intraarterially to limb muscles of nonhuman primates. *Human Gene Therapy*, 12(4), 427–438.
- Vitadello, M., Schiaffino, M. V., Picard, A., Scarpa, M., & Schiaffino, S. (1994). Gene-transfer in regenerating muscle. *Human Gene Therapy*, 5(1), 11–18.
- Doh, S. G., Vahlsing, H. L., Hartikka, J., Liang, X., & Manthorpe, M. (1997). Spatial-temporal patterns of gene expression in mouse skeletal muscle after injection of lacZ plasmid DNA. *Gene Therapy*, 4(7), 648–663.
- Utvik, J. K., Nja, A., & Gundersen, K. (1999). DNA injection into single cells of intact mice. *Human Gene Therapy*, 10(2), 291–300.
- Zador, E., & Wuytack, F. (2003). Expression of SERCA2a is independent of innervation in regenerating soleus muscle. *American Journal of Physiology—Cell Physiology*, 285(4), C853–C861.
- Zádor, E., Fenyvesi, R., & Wuytack, F. (2005). Expression of SERCA2a is not regulated by calcineurin or upon mechanical unloading in skeletal muscle regeneration. *FEBS Letters*, 579(3), 749–752.
- Zador, E. (2008). dnRas stimulates autocrine–paracrine growth of regenerating muscle via calcineurin-NFAT-IL-4 pathway. *Biochemical and Biophysical Research and Communications*, 375(2), 265–270.
- Zádor, E., Owsianik, G., & Wuytack, F. (2011). Silencing SERCA1b in a few fibers stimulates growth in the entire regenerating soleus muscle. *Histochemistry and Cell Biology*, 135(1), 11–20.
- Stickland, N. C. (1983). The arrangement of muscle-fibers and tendons in 2 muscles used for growth-studies. *Journal of Anatomy*, 136(JAN), 175–179.
- Zádor, E., Mandler, L., Ver Heyen, M., Dux, L., & Wuytack, F. (1996). Changes in mRNA levels of the sarcoplasmic/endoplasmic-reticulum Ca(2+)-ATPase isoforms in the rat soleus muscle regenerating from notexin-induced necrosis. *Biochemical Journal*, 320(Pt 1), 107–113.
- Harris, J. B., Johnson, M. A., & Karlsson, E. (1975). Pathological responses of rat skeletal muscle to a single subcutaneous injection of a toxin isolated from the venom of the Australian tiger snake, *Notechis scutatus scutatus*. *Clinical and Experimental Pharmacology and Physiology*, 2(5), 383–404.

20. Tago, H., Kimura, H., & Maeda, T. (1986). Visualization of detailed acetylcholinesterase fiber and neuron staining in rat brain by a sensitive histochemical procedure. *Journal of Histochemistry and Cytochemistry*, *34*(11), 1431–1438.
21. Kopniczky, Z., Dobó, E., Borbély, S., Világi, I., Détári, L., Krisztin-Péva, B., et al. (2005). Lateral entorhinal cortex lesions rearrange afferents, glutamate receptors, increase seizure latency and suppress seizure-induced c-fos expression in the hippocampus of adult rat. *Journal of Neurochemistry*, *95*, 111–124.
22. Hall, Z. W., & Kelly, R. B. (1971). Enzymatic detachment of endplate acetylcholinesterase from muscle. *Nature New Biology*, *232*, 62.
23. McMahan, U. J., Sanes, J. R., & Marshall, L. M. (1978). Cholinesterase is associated with the basal lamina at the neuromuscular junction. *Nature*, *271*, 172–174.
24. Tidball, J. G., Salem, G., & Zernicke, R. (1993). Site and mechanical conditions for failure of skeletal muscle in experimental strain injuries. *Journal of Applied Physiology*, *74*(3), 1280–1286.
25. Maier, A. (1989). Contours and distribution of sites that react with antiacetylcholinesterase in chicken intrafusal fibers. *American Journal of Anatomy*, *185*(1), 33–41.
26. Moss, F. P., & Leblond, C. P. (1971). Satellite cells as the source of nuclei in muscles of growing rats. *Anatomical Record*, *170*(4), 421–435.
27. Vaittinen, S., Hurme, T., Rantanen, J., & Kalimo, H. (2002). Transected myofibres may remain permanently divided in two parts. *Neuromuscular Disorders*, *12*(6), 584–587.
28. Whalen, R. G., Harris, J. B., Butler-Browne, G. S., & Sesodia, S. (1990). Expression of myosin isoforms during notexin-induced regeneration of rat soleus muscles. *Developmental Biology*, *141*(1), 24–40.
29. Frank, E., Jansen, J. K., Lono, T., & Westgaard, R. H. (1975). The interaction between foreign and original motor nerves innervating the soleus muscle of rats. *Journal of Physiology*, *247*(3), 725–743.
30. Brown, M. C., Jansen, J. K., & Van Essen, D. (1976). Polyneuronal innervation of skeletal muscle in new-born rats and its elimination during maturation. *Journal of Physiology*, *261*(2), 387–422.
31. Paul, A. C. (2001). Muscle length affects the architecture and pattern of innervation differently in leg muscles of mouse, guinea pig, and rabbit compared to those of human and monkey muscles. *Anatomical Record*, *262*(3), 301–309.
32. Grubb, B. D., Harris, J. B., & Schofield, I. S. (1991). Neuromuscular transmission at newly formed neuromuscular junctions in the regenerating soleus muscle of the rat. *Journal of Physiology*, *441*(1), 405–421.
33. Rana, Z. A., Ekmark, M., & Gundersen, K. (2004). Coexpression after electroporation of plasmid mixtures into muscle in vivo. *Acta Physiologica Scandinavica*, *181*(2), 233–238.
34. Davis, C. E., Harris, J. B., & Nicholson, L. V. B. (1991). Myosin isoform transitions and physiological properties of regenerated and re-innervated soleus muscles of the rat. *Neuromuscular Disorder*, *1*(6), 411–421.
35. Bureau, M. F., Naimi, S., Torero Ibad, R., Seguin, J., Georger, C., Arnould, E., et al. (2004). Intramuscular plasmid DNA electrotransfer: Biodistribution and degradation. *Biochimica Et Biophysica Acta (BBA)—Gene Structure and Expression*, *1676*(2), 138–148.
36. Snow, M. H. (1978). An autoradiographic study of satellite cell differentiation into regenerating myotubes following transplantation of muscles in young rats. *Cell and Tissue Research*, *186*(3), 535–540.
37. Robertson, T. A., Papadimitriou, J. M., & Grounds, M. D. (1993). Fusion of myogenic cells to the newly sealed region of damaged myofibres in skeletal muscle regeneration. *Neuropathology and Applied Neurobiology*, *19*(4), 350–358.
38. Horsley, V., Friday, B. B., Matteson, S., Kegley, K. M., Gephart, J., & Pavlath, G. K. (2001). Regulation of the growth of multinucleated muscle cells by an Nfatc2-dependent pathway. *Journal of Cell Biology*, *153*(2), 329–338.
39. Bruusgaard, J. C., Liestøl, K., Ekmark, M., Kollstad, K., & Gundersen, K. (2003). Number and spatial distribution of nuclei in the muscle fibres of normal mice studied in vivo. *Journal of Physiology*, *551*(2), 467–478.
40. Morgan, J. E., & Partridge, T. A. (2003). Muscle satellite cells. *International Journal of Biochemistry & Cell Biology*, *35*, 1151–1156.
41. Bevan, S., & Steinbach, J. H. (1977). The distribution of  $\alpha$ -bungarotoxin binding sites on mammalian skeletal muscle developing in vivo. *Journal of Physiology*, *267*, 195–213.
42. Mendler, L., Zádor, E., Dux, L., & Wuytack, F. (1998). mRNA levels of myogenic regulatory factors in rat slow and fast muscles regenerating from notexin-induced necrosis. *Neuromuscular Disorder*, *8*, 533–541.